

Hidehiko Okazawa and Yu-Kyeong Kim

---

## Cerebrovascular Disease and O-15 PET

### Measurement of Hemodynamic Parameters Using O-15 PET

Positron emission tomography (PET) and O-15 tracers have been used for greater than 30 years to evaluate human cerebral hemodynamics in patients with cerebral vascular disease (CVD). Quantitative measurement of cerebral blood flow (CBF) and metabolism is important because critical impairment of cerebral circulation induces irreversible damage to the cerebral cortex, causing neuronal deficits or functional damage. The cerebral regions of impaired hemodynamics, “misery perfusion” are visualized by mismatch between oxygen metabolism and CBF [1, 2], which is usually delineated by the elevation of oxygen extraction fraction (OEF) in O-15 gas PET [2–6]. Because patients with misery perfusion show a significantly higher incidence rate of stroke or recurrent stroke [7–9], evaluation of

hemodynamic status in CVD patients is very important to determine indication of neurosurgical treatment. To quantitatively evaluate cerebral hemodynamic status, methods for precise measurement were developed and its accuracy has also been improved with the progression of PET scanner resolution.

The historic development of PET measurement of cerebral hemodynamic parameters is shown in Table 14.1 [10–25]. The impaired hemodynamic status of misery perfusion was at first determined using a count-based semiquantitative method [1, 2]. Quantitative methods for cerebral circulation and oxygen metabolism were proposed in the early 1980s, and the two common methods based on a single compartment model are known as the steady-state method and the bolus inhalation method (so-called ‘autoradiographic’ or ‘three-step’ method) (Fig. 14.1a). A quantitative steady-state method with continuous inhalation of O-15 labeled gases such as  $^{15}\text{O}_2$ ,  $\text{C}^{15}\text{O}_2$  and  $\text{C}^{15}\text{O}$  was proposed [15, 16]. Lammertsma et al. corrected the effect of cerebral blood volume (CBV) on OEF in the O-15 gas steady-state method [17]. OEF is usually overestimated when CBV correction is not applied. Although this method is simple and easier than the bolus tracer administration method, specific equipment must be installed to keep radioactive gas at a constant rate of concentration during PET scans, and patients cannot avoid high exposure to radioactive gas. The autoradiographic method developed for measurement of CBF using O-15 water was applied [18, 19] to

---

H. Okazawa, M.D., Ph.D. (✉)

Division of Biomedical Imaging, The Faculty of Medical Sciences, University of Fukui, Fukui 910-1193, Japan  
e-mail: okazawa@u-fukui.ac.jp

Y.-K. Kim, M.D., Ph.D.

Department of Nuclear Medicine, Seoul National University, Bundang Hospital, Gyeonggi-Do 463-707, South Korea  
e-mail: yk3181@snu.ac.kr

**Table 14.1** Measurements of CBF and oxygen metabolism using O-15 tracers

Authors	Tracers	Method	Parameters	Year	References
Ter-Pogossian et al., Raichle et al.	H <sub>2</sub> <sup>15</sup> O, <sup>15</sup> O <sub>2</sub>	Bolus (No. image)	CBF, CMRO <sub>2</sub>	1969–1976	[10–13]
Jones et al.	<sup>15</sup> O <sub>2</sub> , C <sup>15</sup> O <sub>2</sub>	Steady-state	Qualitative	1976	[14]
Frackowiak et al., Lammertsma et al.	<sup>15</sup> O <sub>2</sub> , C <sup>15</sup> O <sub>2</sub>	Steady-state	CBF, OEF, CMRO <sub>2</sub>	1980, 1981	[15, 16]
Lammertsma et al.	<sup>15</sup> O <sub>2</sub> , C <sup>15</sup> O	Steady-state(OEF-CBV correction)	OEF, CMRO <sub>2</sub>	1983	[17]
Herscovitch et al., Raichle et al.	H <sub>2</sub> <sup>15</sup> O	Bolus, (ARG)	CBF	1983	[18, 19]
Mintun et al.	H <sub>2</sub> <sup>15</sup> O, <sup>15</sup> O <sub>2</sub> , C <sup>15</sup> O	Bolus, (3-step)	CBF, CBV, OEF, CMRO <sub>2</sub>	1984	[20]
Lammertsma et al.	<sup>11</sup> CO, <sup>11</sup> C-HSA	Equilibrium	CBV, Htc ratio	1984	[21]
Gambhir et al.	H <sub>2</sub> <sup>15</sup> O	Bolus, (2-CM)	CBF, V <sub>d</sub>	1987	[22]
Lammertsma et al.	C <sup>15</sup> O <sub>2</sub>	Build-up	CBF	1989	[23]
Ohta et al.	<sup>15</sup> O <sub>2</sub> , H <sub>2</sub> <sup>15</sup> O	Bolus, (1-step, 2-CM)	CMRO <sub>2</sub> , OEF, CBF, V <sub>0</sub>	1992, 1996	[24, 25]

CBF cerebral blood flow, CMRO<sub>2</sub> cerebral metabolic rate of oxygen, OEF oxygen extraction fraction, CBV cerebral blood volume, V<sub>d</sub> distribution volume, Htc ratio cerebral-to-large vessel hematocrit ratio, V<sub>0</sub> arterial-to-capillary volume, ARG autoradiographic method, CM compartment model

the measurement of oxygen metabolism with bolus administration of O-15 tracers (three-step method) [20]. This method does not require the specific equipment to maintain a constant concentration rate of radioactive gas.

Because various quantitative methods for measurement of CBF using O-15 water PET were proposed, the method for quantitative measurement was improved, as well as several methods for image calculation and correction of parameters to improve the image quality and calculation time [25–35]. A two-compartment (one-tissue compartment) model analysis increased the accuracy of CBF values by separating the vascular component from the blood flow value as shown in the following equation (Fig. 14.1b) [24, 25]:

$$C_b(t) = K_1 \cdot C_a(t) \otimes e^{-k_2 t} + V_0 \cdot C_a(t).$$

where C<sub>b</sub>(t) and C<sub>a</sub>(t) are the concentrations of tracer in the brain and arteries, K<sub>1</sub> and k<sub>2</sub> are rate constants, V<sub>0</sub> is arterial-to-capillary blood volume, and ⊗ denotes operation of convolution. A single-compartment model analysis can be described with elimination of the second

term in this equation [18, 19]. Rate constant of K<sub>1</sub> linearly correlates with blood flow, which can be corrected by extraction of the tracer (K<sub>1</sub> = E · F; E = extraction, F = blood flow). If this method is applied to the bolus <sup>15</sup>O<sub>2</sub> inhalation method, the cerebral metabolic rate of oxygen (CMRO<sub>2</sub>) can be calculated without measuring CBF and CBV by the equation of CMRO<sub>2</sub> = tO<sub>2</sub>c · K<sub>1</sub>, where tO<sub>2</sub>c is total arterial O<sub>2</sub> content (one-step method) [24]. This method includes an assumption that the metabolized and recirculating radioactivity of O-15 water is negligible during the scanning time. The CMRO<sub>2</sub> values tend to be overestimated because of this assumption as well as the fact that venous radioactivity cannot be eliminated completely despite separation of V<sub>0</sub> [24, 36]. This simple method, however, can evaluate changes in oxygen metabolism during neural stimulation by repeated measurement of CMRO<sub>2</sub> in activation studies [37]. Recently, a report from 11 PET centers in Japan, in which several representative methods for O-15 PET were used, showed no significant differences in quantitative values of hemodynamic parameters among the methods [38]. In this study, overall mean ± SD (standard deviation) values in

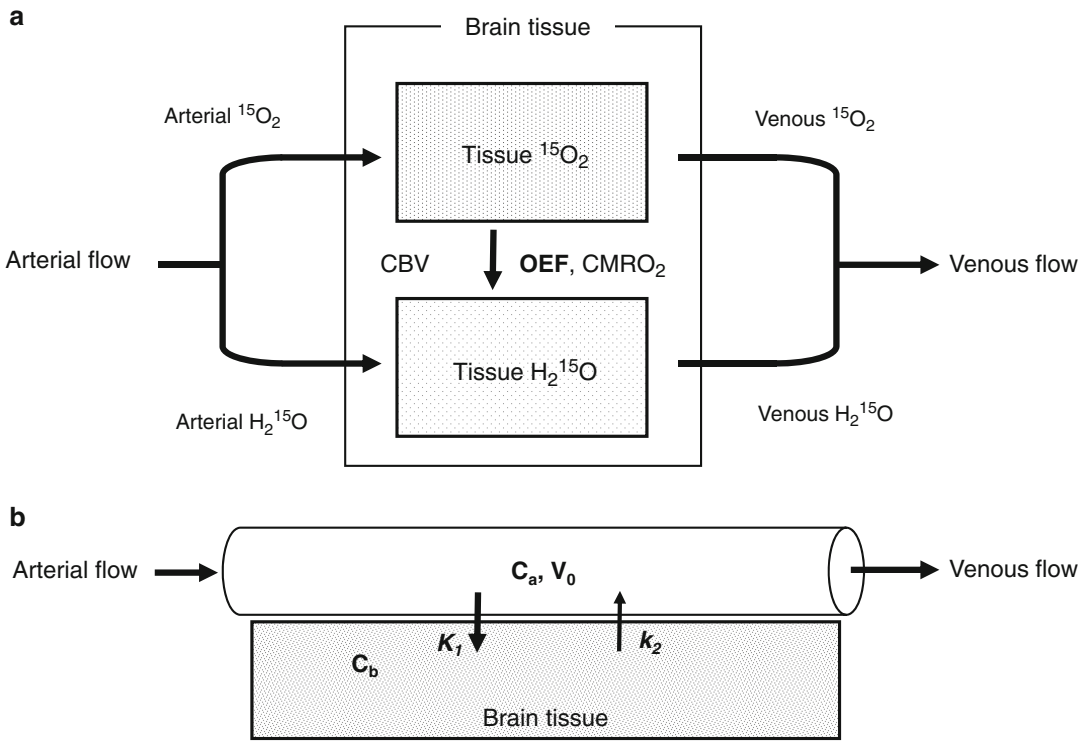


**Fig. 14.1** Schematic of one-compartment (a) and two-compartment (one-tissue compartment) (b) models for calculation of CBF and oxygen metabolism. In model (a), CBF calculation using  $\text{H}_2^{15}\text{O}$  or  $\text{C}^{15}\text{O}_2$  can be explained by

neglecting  $^{15}\text{O}_2$  elements.  $C_a$  and  $C_b$  are the concentrations of arterial and brain tissue radioactivity,  $K_1$  and  $k_2$  are rate constants of tracers, and  $V_0$  is the arterial-to-capillary blood volume

cerebral cortical regions for healthy human subjects were  $\text{CBF} = 44.4 \pm 6.5 \text{ mL}/100 \text{ g}/\text{min}$ ,  $\text{CBV} = 3.8 \pm 0.7 \text{ mL}/100 \text{ g}$ ,  $\text{CMRO}_2 = 3.3 \pm 0.5 \text{ mL}/100 \text{ g}/\text{min}$ , and  $\text{OEF} = 0.44 \pm 0.06$ .

Contrary to the development of precise quantification methods, one long-term prospective study reported that the diagnostic accuracy for misery perfusion was similar to, or rather, better with the count-based method compared with the quantitative evaluation [39, 40]. Recent reports on the application of count-based semi-quantitative methods have been controversial. A normalized method using cerebellar counts showed poor agreement with quantitative OEF elevation [41]. However, another study employing a simplified ipsilateral-to-contralateral asymmetry index (AI) comparison method using count-based ratio images showed good accordance with the AI of quantitative OEF in CVD patients [42, 43]. The advantage of these

simplified methods is that the scanning protocol is simple and the procedure is noninvasive without arterial blood sampling. For precise evaluation of hemodynamic changes in the brain, quantitative methods with arterial blood sampling are required; however, in clinical studies, the simplified method is preferable for assessment of the hemodynamic status.

## Chronic Cerebrovascular Disease

CBF autoregulation is the mechanism by which CBF is maintained during changes in systemic blood pressure. This physiologic function also can be applied to the relationship between changes in cerebral perfusion pressure (CPP) and CBF. CBF is maintained by autoregulatory vasoconstriction and vasodilatation of arterioles when CPP is changed; however, CBF decreases when

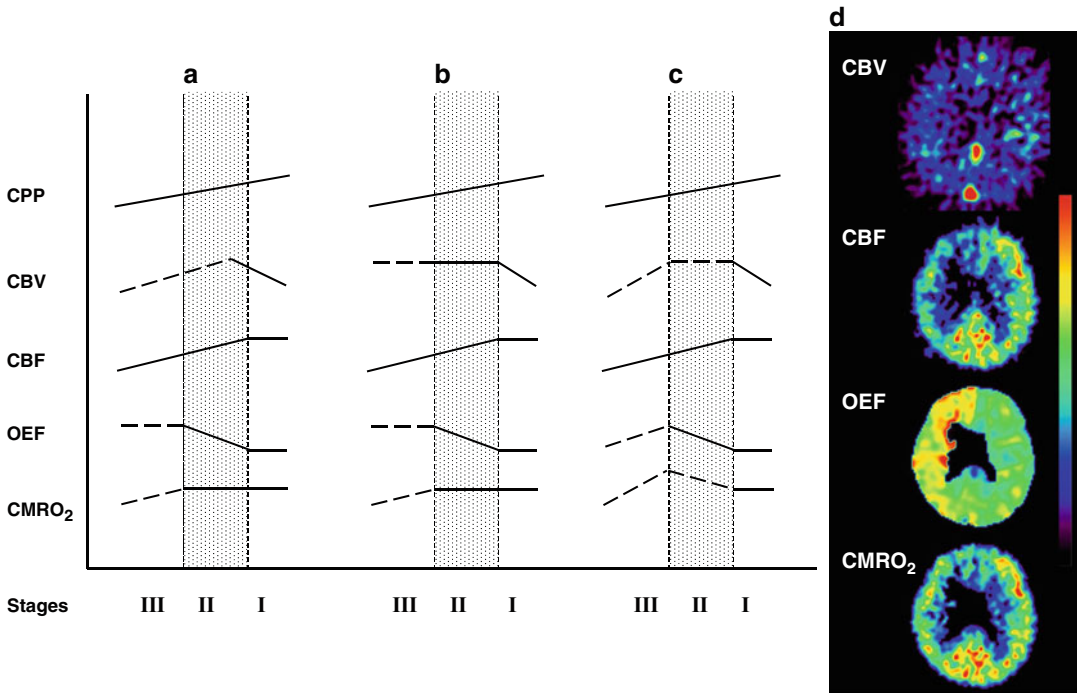


**Fig. 14.2** Graph explaining changes in hemodynamic parameters induced by decreases in perfusion pressure (CPP). Powers et al. initially proposed the basic concept of hypothesis (a), and later revised the model with a minor change in CBV (b) [3–6, 40, 46]. Nemoto et al. modified this model based on their two-compartment

analysis (c) [47]. Dotted area in the graph shows stage II impairment. Representative PET images for patients with misery perfusion (stage II) are presented in the right column (d). Misery perfusion shows a slight decrease in CMRO<sub>2</sub> at the region of CBF decrease and OEF elevation

CPP decreases below the lower limit of autoregulation (Fig. 14.2). Experiments on cerebrovascular autoregulation have shown an increase in the diameter of resistance arteries as a function of the decrease in systemic blood pressure [44, 45]. Although this vasodilatory change caused by a reduction in blood pressure is a well-known physiologic reaction in the acute phase, it is not clear whether the cerebral circulation in patients with chronic CVD shows similar vasodilatory compensation in the resistance arteries. To explain the cerebral hemodynamic changes in CVD patients, Powers et al. originally presumed that the dilatory change in resistance vessels continues even after the vasodilatation can no longer compensate for CBF autoregulation as described in animal experiments (Fig. 14.2a) [3, 5, 6]. They later modified this model with respect to hemo-

dynamics in chronic CVD patients (Fig. 14.2b) [39, 46] and reported the importance of neurosurgical treatment for stage II ischemia. Recently, Nemoto et al. slightly corrected this hemodynamic assumption based on their analysis using a two-compartment model (Fig. 14.2c) [47]. However, most patients with misery perfusion usually show a slight decrease in CMRO<sub>2</sub> (Fig. 14.2d) as described by Powers et al. in their reports [3–5].

Several researchers and neurosurgeons reported that the extracranial-to-intracranial (EC/IC) bypass surgery is efficient for patients with misery perfusion caused by cerebral arterial occlusive lesions [3–6, 48]. However, the multi-center cohort study conducted in the mid-1980s for evaluation of prognosis of CVD patients contradicted the effectiveness of the EC/IC bypass

surgery [49, 50]. The problem with the cohort study performed by the EC/IC bypass surgery group was that patient entry criteria were inappropriate. All patients with stenotic lesions in the internal carotid arteries were involved in the study, and there was no significant difference in outcome between the surgical treatment and simple medication groups. However, as many recent studies have suggested, if the patients do not show neurologic symptoms, stenocclusive lesions do not necessarily cause hemodynamic impairment that may induce strokes in the brain [51–53]. Several long-term prospective studies have shown that patients without hemodynamic deficiency did not have a high incidence of subsequent infarction compared with those with misery perfusion. In their 5-year follow-up study ( $n=40$ ), Yamauchi et al. (Kyoto University group) showed that the recurrence rate of stroke was significantly higher in patients with misery perfusion (57.1%) compared with those without OEF elevation (18.2%) [7, 8]. Grubb et al. (Washington University group) also showed a similar result with a larger patient sample ( $n=81$ ) and 3-year follow-up period [9]. Their results suggest that a patient with stenocclusive lesions in major cerebral arteries may not show neurologic deficits or hemodynamic impairment if the lesion advances slowly enough to generate sufficient collateral circulation.

This evidence shows the importance of evaluation of the cerebral circulation and oxygen metabolism; however, the degree of hemodynamic impairment can be evaluated by a reduction of cerebral vasoreactivity (CVR) after acetazolamide (ACZ) or  $\text{CO}_2$  loading [54–56]. The vasodilatory effect of ACZ or  $\text{CO}_2$  without changes in systemic blood pressure causes increases in CBF in normal circulation [54, 57, 58]. Recently, several long-term prospective studies were conducted using the quantitative measurement of baseline CBF and CVR to confirm the risk of developing cerebral infarction in hemodynamic impairment [59–67]. The studies were performed to contradict the prospective cohort study that denied the effectiveness and benefits of EC/IC bypass surgery for patients with cerebral arterial occlusion. The aim of the studies was to prove that symptomatic patients with CVD who

have hemodynamic impairment should be treated by surgical or interventional methods to avoid recurrent strokes. The studies with alternative methods reported a benefit of measuring CVR to evaluate the hemodynamic condition and to predict the risk of subsequent strokes [59–64]. On the other hand, nonquantitative evaluation of CVR failed to predict any significant difference in recurrent stroke risk between normal and impaired CVR groups [65–67]. A recent study reported that diagnostic accuracy for detecting misery perfusion by using quantitative measurement of CBF and CVR after ACZ administration had a sensitivity of 56.3%, specificity of 88.2%, and accuracy of 78.0% [68].

Figures 14.3 and 14.4 show representative cases of stage I and stage II hemodynamic impairment. A patient with stage I showed a decrease in CVR without elevation of OEF (Fig. 14.3), while a patient with misery perfusion (stage II impairment) showed elevation of OEF as well as a decrease in CVR in the affected hemisphere.

---

### Evaluation of Cerebral Glucose Metabolism Following Stroke

Stroke is caused by a variety of pathologic changes that produce a focal reduction of blood flow or multifocal regions of compromised perfusion. In most of these cases, the end result of reduced CBF and inadequate delivery of oxygen and glucose to the brain is cerebral infarction [69]. In stabilized infarction, [ $^{18}\text{F}$ ]2-fluoro-2-deoxy-D-glucose (FDG) PET shows a focal area of hypometabolism in a location consistent with focal cerebral infarction [70]. However, the metabolic impairment in stroke patients is not limited to the area of infarction. PET and single-photon emission computed tomography studies have demonstrated remote effects in regional CBF and metabolism consequent to focal infarction [71]. From the early period after an acute brain lesion, diaschisis can develop because of reduced cerebral function resulting from the interruption of normal input to a region not directly involved in the stroke. Distinguishing between regional ischemia and depressed neurometabolic activity is

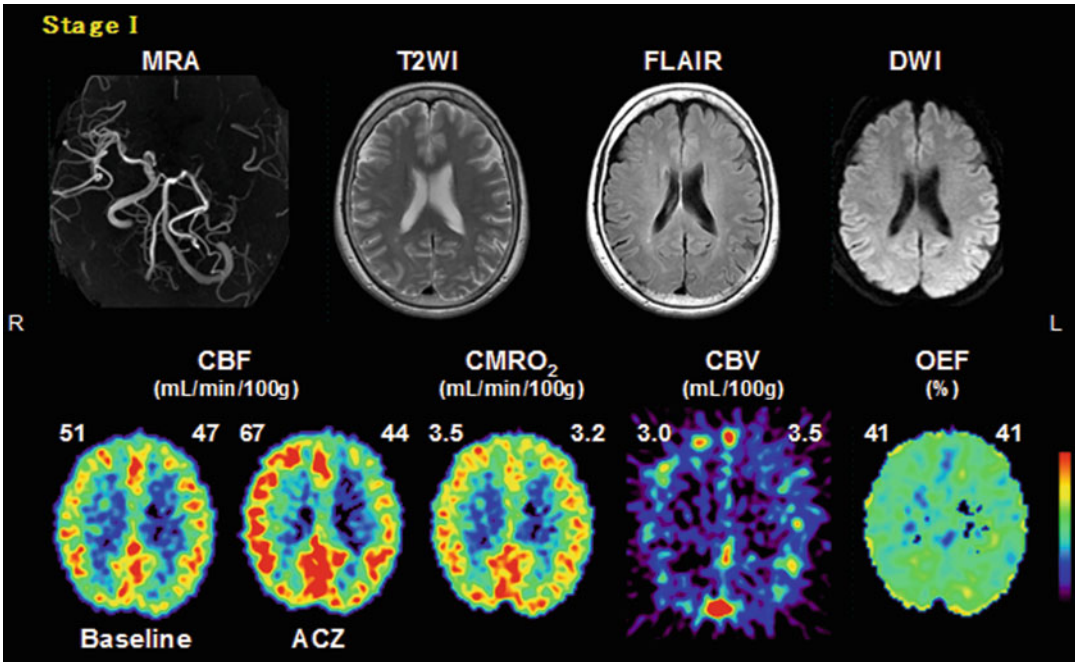


**Fig. 14.3** A representative case of a stage I patient with stenosis in the left MCA. CBF and CMRO<sub>2</sub> did not show a significant decrease in the affected hemisphere, but CVR

after ACZ administration showed the lack of vascular reactivity. Numbers are quantitative values for each hemisphere MRA: MR angiography

aided by the calculation of OEF with CMRO<sub>2</sub> and cerebral metabolism [48, 72, 73]. In the regions of diaschisis, the metabolic rate as measured by local glucose consumption was decreased, while OEF and CMRO<sub>2</sub> are preserved. Although there are reports of ischemic penumbra and luxury perfusion persisting after stroke [74, 75], normal oxygen extraction surrounding stroke suggests diaschisis [76].

It is likely that diaschisis is associated with functional impairment can determine the severity of the clinical images in the acute stage and its recovery [77]. Diaschisis can occur in the areas surrounding the “infarcted” lesion, in the outside of the lesion in the affected hemisphere as well as in the other hemisphere (e.g., “cross hemispheric” or “cross callosal” diaschisis). A regression of diaschisis is usually, although not invariably, found in the following months and may be related to the clinical recovery [78]. Immediately following stroke, extensive functional depression measured by glucose consumption and associated functional impairment can develop in the

bilateral hemisphere [71, 79, 80]. In many reports, the improvement in function after left middle cerebral artery (MCA) stroke, e.g., progression from hand and leg weakness with aphasia to only hand weakness has been observed and seems linked to the anatomy adjacent to the cerebral infarction. Cortical diaschisis is particularly prominent with thalamic infarcts which often lead to pronounced thalamocortical diaschisis with corresponding cognitive deficits [81, 82]. In patients with cortical or subcortical infarction involved in the language area, regression of intrahemispheric and transhemispheric diaschisis may be associated with the recovery of a function that is subserved by an extensive network of interconnected regions in both hemispheres, at least in the first 6 months following stroke [78]. However, in cases of crossed (contralateral) cerebellar diaschisis (CCD) which can occur early after supratentorial ischemic lesions, particularly in the basal ganglia or frontal or parietal cortex, CCD can persist over a long period of time with eventual cerebellar atrophy, but usually lacks

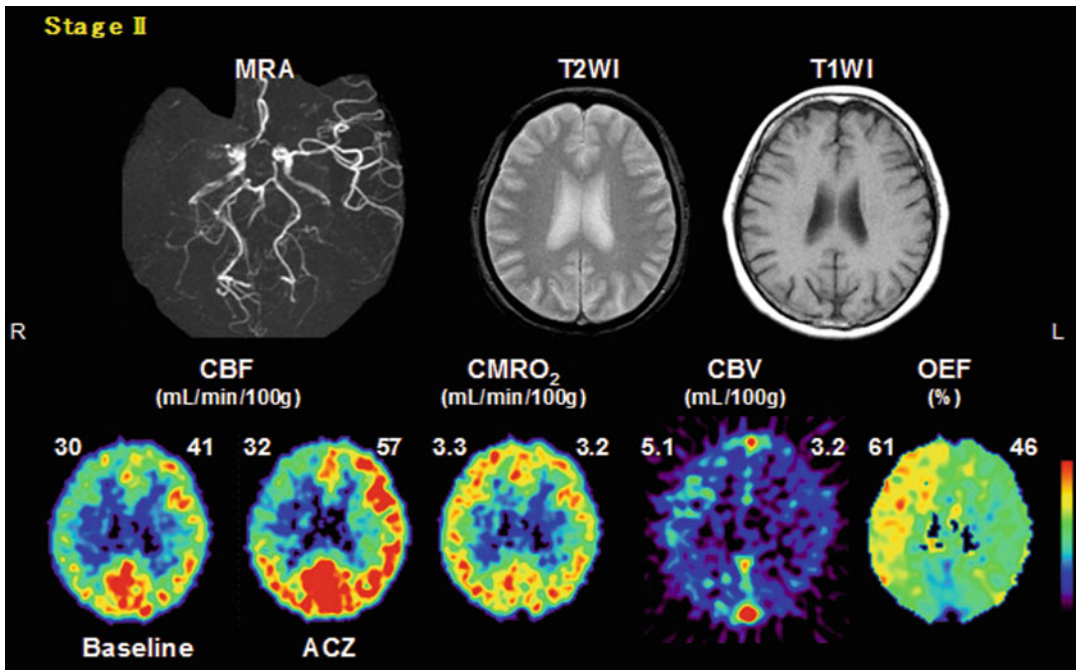


**Fig. 14.4** A representative case of chronic CVD with misery perfusion (stage II) in the right cerebral hemisphere as a result of right MCA occlusion (see MRA).

This patient did not show decrease in  $CMRO_2$  in the impaired region (*right* frontal lobe). Numbers are quantitative values for each hemisphere

major correlates in neurologic functional impairment. The regional glucose metabolism in diaschisis in the early period following stroke may be associated with functional improvement during the recovery phase [83, 84]. Cerebral glucose metabolism in the left hemisphere outside the infarcted region, particularly temporoparietal metabolism, in the acute stage following stroke in the left hemisphere is thought to be the best predictor of recovery of auditory comprehension [85], and suggests an important role for intra-hemispheric diaschisis in determining the severity of the clinical picture in the acute stage and its recovery [86].

Bilateral temporoparietal glucose metabolism shows a positive correlation with auditory comprehensive function in patients with aphasia following stroke.

Besides of the resolution of diaschisis, reorganization in the brain plays an important role in poststroke functional recovery. Changes in regional glucose metabolism in the contralateral

hemisphere associated with poststroke reorganization have been detected by FDG PET [83]. The parallel change in glucose metabolism and high-energy phosphate metabolism associated with poststroke functional recovery is possibly explained by cerebral reorganization in the contralateral premotor cortex. The resulting cerebral reorganization may account for improved patient functional recovery from stroke. Similar findings can be observed in patients with aphasia following stroke. The changes in neuronal activities measured by glucose metabolism in the surrounding area of the “infarcted” region, in the contralateral mirror area and left Broca’s area during activation were highly predictive of the recovery of auditory comprehension, indicating that the possibility to activate an extensive, bihemispheric neural network was crucial for recovery [84]. Hypermetabolism, measured by increased FDG uptake in the contralateral homologous area, indicates that there is increased energy being used, possibly because of increased neuronal plasticity.

## References

- Lenzi GL, Jones T, McKenzie CG, Moss S. Non-invasive regional study of chronic cerebrovascular disorders using the oxygen-15 inhalation technique. *J Neurol Neurosurg Psychiatry*. 1978;41:11–7.
- Baron JC, Boussier MG, Rey A, Guillard A, Comar D, Castaigne P. Reversal of focal “misery-perfusion syndrome” by extra-intracranial arterial bypass in hemodynamic cerebral ischemia. A case study with  $^{15}\text{O}$  positron emission tomography. *Stroke*. 1981; 12:454–9.
- Powers WJ, Grubb Jr RL, Raichle ME. Physiological responses to focal cerebral ischemia in humans. *Ann Neurol*. 1984;16:546–52.
- Powers WJ, Raichle ME. Positron emission tomography and its application to the study of cerebrovascular disease in man. *Stroke*. 1985;16:361–76.
- Powers WJ, Press GA, Grubb Jr RL, Gado M, Raichle ME. The effect of hemodynamically significant carotid artery disease on the hemodynamic status of the cerebral circulation. *Ann Intern Med*. 1987; 106:27–34.
- Powers WJ. Cerebral hemodynamics in ischemic cerebrovascular disease. *Ann Neurol*. 1991; 29:231–40.
- Yamauchi H, Fukuyama H, Nagahama Y, Nabatame H, Nakamura K, Yamamoto Y, et al. Evidence of misery perfusion and risk for recurrent stroke in major cerebral arterial occlusive diseases from PET. *J Neurol Neurosurg Psychiatry*. 1996;61:18–25.
- Yamauchi H, Fukuyama H, Nagahama Y, Nabatame H, Ueno M, Nishizawa S, et al. Significance of increased oxygen extraction fraction in five-year prognosis of major cerebral arterial occlusive diseases. *J Nucl Med*. 1999;40:1992–8.
- Grubb Jr RL, Derdeyn CP, Fritsch SM, Carpenter DA, Yundt KD, Videen TO, et al. Importance of hemodynamic factors in the prognosis of symptomatic carotid occlusion. *JAMA*. 1998;280:1055–60.
- Ter-Pogossian MM, Eichling JO, Davis DO, Welch MJ, Metzger JM. The determination of regional cerebral blood flow by means of water labeled with radioactive oxygen 15. *Radiology*. 1969;93:31–40.
- Ter-Pogossian MM, Eichling JO, Davis DO, Welch MJ. The measure in vivo of regional cerebral oxygen utilization by means of oxyhemoglobin labeled with radioactive oxygen-15. *J Clin Invest*. 1970;49:381–91.
- Raichle ME, Grubb Jr RL, Gado MH, Eichling JO, Ter-Pogossian MM. Correlation between regional cerebral blood flow and oxidative metabolism. In vivo studies in man. *Arch Neurol*. 1976;33:523–6.
- Raichle ME, Grubb Jr RL, Eichling JO, Ter-Pogossian MM. Measurement of brain oxygen utilization with radioactive oxygen-15: experimental verification. *J Appl Physiol*. 1976;40:638–40.
- Jones T, Chesler DA, Ter-Pogossian MM. The continuous inhalation of oxygen-15 for assessing regional oxygen extraction in the brain of man. *Br J Radiol*. 1976;49:339–43.
- Frackowiak RS, Lenzi GL, Jones T, Heather JD. Quantitative measurement of regional cerebral blood flow and oxygen metabolism in man using  $^{15}\text{O}$  and positron emission tomography: theory, procedure, and normal values. *J Comput Assist Tomogr*. 1980;4:727–36.
- Lammertsma AA, Jones T, Frackowiak RS, Lenzi GL. A theoretical study of the steady-state model for measuring regional cerebral blood flow and oxygen utilization using oxygen-15. *J Comput Assist Tomogr*. 1981;5:544–50.
- Lammertsma AA, Wise RJ, Heather JD, Gibbs JM, Leenders KL, Frackowiak RS, et al. Correction for the presence of intravascular oxygen-15 in the steady-state technique for measuring regional oxygen extraction ratio in the brain: 2. Results in normal subjects and brain tumour and stroke patients. *J Cereb Blood Flow Metab*. 1983;3:425–31.
- Herscovitch P, Markham J, Raichle ME. Brain blood flow measured with intravenous  $\text{H}_2^{15}\text{O}$ . I. Theory and error analysis. *J Nucl Med*. 1983;24:782–9.
- Raichle ME, Martin WR, Herscovitch P, Mintun MA, Markham J. Brain blood flow measured with intravenous  $\text{H}_2^{15}\text{O}$ . II. Implementation and validation. *J Nucl Med*. 1983;24:790–8.
- Mintun MA, Raichle ME, Martin WR, Herscovitch P. Brain oxygen utilization measured with O-15 radiotracers and positron emission tomography. *J Nucl Med*. 1984;25:177–87.
- Lammertsma AA, Brooks DJ, Beaney RP, Turton DR, Kensett MJ, Heather JD, et al. In vivo measurement of regional cerebral haematocrit using positron emission tomography. *J Cereb Blood Flow Metab*. 1984; 4:317–22.
- Gambhir SS, Huang SC, Hawkins RA, Phelps ME. A study of the single compartment tracer kinetic model for the measurement of local cerebral blood flow using  $^{15}\text{O}$ -water and positron emission tomography. *J Cereb Blood Flow Metab*. 1987;7:13–20.
- Lammertsma AA, Frackowiak RS, Hoffman JM, Huang SC, Weinberg IN, Dahlbom M, et al. The  $\text{C}^{15}\text{O}_2$  build-up technique to measure regional cerebral blood flow and volume of distribution of water. *J Cereb Blood Flow Metab*. 1989;9:461–70.
- Ohta S, Meyer E, Thompson CJ, Gjedde A. Oxygen consumption of the living human brain measured after a single inhalation of positron emitting oxygen. *J Cereb Blood Flow Metab*. 1992;12:179–92.
- Ohta S, Meyer E, Fujita H, Reutens DC, Evans A, Gjedde A. Cerebral [ $^{15}\text{O}$ ]water clearance in humans determined by PET: I. Theory and normal values. *J Cereb Blood Flow Metab*. 1996;16:765–80.
- Herscovitch P, Raichle ME. Effect of tissue heterogeneity on the measurement of cerebral blood flow with the equilibrium  $\text{C}^{15}\text{O}_2$  inhalation technique. *J Cereb Blood Flow Metab*. 1983;3:407–15.
- Alpert NM, Eriksson L, Chang JY, Bergstrom M, Litton JE, Correia JA, et al. Strategy for the measure-



- ment of regional cerebral blood flow using short-lived tracers and emission tomography. *J Cereb Blood Flow Metab.* 1984;4:28–34.
28. Carson RE, Huang SC, Green MV. Weighted integration method for local cerebral blood flow measurements with positron emission tomography. *J Cereb Blood Flow Metab.* 1986;6:245–58.
  29. Huang SC, Feng DG, Phelps ME. Model dependency and estimation reliability in measurement of cerebral oxygen utilization rate with oxygen-15 and dynamic positron emission tomography. *J Cereb Blood Flow Metab.* 1986;6:105–19.
  30. Koeppe RA, Holden JE, Ip WR. Performance comparison of parameter estimation techniques for the quantitation of local cerebral blood flow by dynamic positron computed tomography. *J Cereb Blood Flow Metab.* 1985;5:224–34.
  31. Iida H, Kanno I, Miura S, Murakami M, Takahashi K, Uemura K. Error analysis of a quantitative cerebral blood flow measurement using  $H_2^{15}O$  autoradiography and positron emission tomography, with respect to the dispersion of the input function. *J Cereb Blood Flow Metab.* 1986;6:536–45.
  32. Iida H, Kanno I, Miura S, Murakami M, Takahashi K, Uemura K. A determination of the regional brain/ blood partition coefficient of water using dynamic positron emission tomography. *J Cereb Blood Flow Metab.* 1989;9:874–85.
  33. Cunningham VJ, Jones T. Spectral analysis of dynamic PET studies. *J Cereb Blood Flow Metab.* 1993;13:15–23.
  34. Kimura Y, Hsu H, Toyama H, Senda M, Alpert NM. Improved signal-to-noise ratio in parametric images by cluster analysis. *Neuroimage.* 1999;9:554–61.
  35. Shidahara M, Watabe H, Kim KM, Kudomi N, Ito H, Iida H. Optimal scan time of oxygen-15-labeled gas inhalation autoradiographic method for measurement of cerebral oxygen extraction fraction and cerebral oxygen metabolic rate. *Ann Nucl Med.* 2008; 22:667–75.
  36. Okazawa H, Yamauchi H, Sugimoto K, Takahashi M, Toyoda H, Kishibe Y, et al. Quantitative comparison of the bolus and steady-state methods for measurement of cerebral perfusion and oxygen metabolism: PET study using  $^{15}O$ -gas and water. *J Cereb Blood Flow Metab.* 2001;21:793–803.
  37. Vafaee MS, Meyer E, Marrett S, Paus T, Evans AC, Gjedde A. Frequency-dependent changes in cerebral metabolic rate of oxygen during activation of human visual cortex. *J Cereb Blood Flow Metab.* 1999;19:272–7.
  38. Ito H, Kanno I, Kato C, Sasaki T, Ishii K, Ouchi Y, et al. Database of normal human cerebral blood flow, cerebral blood volume, cerebral oxygen extraction fraction and cerebral metabolic rate of oxygen measured by positron emission tomography with  $^{15}O$ -labelled carbon dioxide or water, carbon monoxide and oxygen: a multicentre study in Japan. *Eur J Nucl Med Mol Imag.* 2004;31:635–43.
  39. Derdeyn CP, Videen TO, Simmons NR, Yundt KD, Fritsch SM, Grubb RL, et al. Count-based PET method for predicting ischemic stroke in patients with symptomatic carotid arterial occlusion. *Radiology.* 1999;212:499–506.
  40. Derdeyn CP, Videen TO, Grubb Jr RL, Powers WJ. Comparison of PET oxygen extraction fraction methods for the prediction of stroke risk. *J Nucl Med.* 2001;42:1195–7.
  41. Ibaraki M, Shimosegawa E, Miura S, Takahashi K, Ito H, Kanno I, et al. PET measurements of CBF, OEF, and CMRO<sub>2</sub> without arterial sampling in hyperacute ischemic stroke: method and error analysis. *Ann Nucl Med.* 2004;18:35–44.
  42. Kobayashi M, Okazawa H, Tsuchida T, Kawai K, Fujibayashi Y, Yonekura Y. Diagnosis of misery perfusion using noninvasive O-15 gas PET. *J Nucl Med.* 2006;47:1581–6.
  43. Kobayashi M, Kudo T, Tsujikawa T, Isozaki M, Arai Y, Fujibayashi Y, et al. Shorter examination method for the diagnosis of misery perfusion using count-based OEF elevation in  $^{15}O$ -gas PET. *J Nucl Med.* 2008;49:242–6.
  44. Grubb Jr RL, Phelps ME, Raichle ME, Ter-Pogassian MM. The effect of arterial blood pressure on the regional cerebral blood volume by x-ray fluorescence. *Stroke.* 1973;4:390–9.
  45. MacKenzie ET, Farrar JK, Fitch W, Graham DI, Gregory PC, Harper AM. Effects of hemorrhagic hypotension on the cerebral circulation. I. Cerebral blood flow and pial arteriolar caliber. *Stroke.* 1979;10:711–8.
  46. Derdeyn CP, Grubb Jr RL, Powers WJ. Cerebral hemodynamic impairment: methods of measurement and association with stroke risk. *Neurology.* 1999;53:251–9.
  47. Nemoto EM, Yonas H, Kuwabara H, Pindzola RR, Sashin D, Meltzer CC, et al. Identification of hemodynamic compromise by cerebrovascular reserve and oxygen extraction fraction in occlusive vascular disease. *J Cereb Blood Flow Metab.* 2004;24:1081–9.
  48. Baron JC, Boussier MG, Comar D, Soussaline F, Castaigne P. Noninvasive tomographic study of cerebral blood flow and oxygen metabolism in vivo. Potentials, limitations, and clinical applications in cerebral ischemic disorders. *Eur Neurol.* 1981;20:273–84.
  49. The EC/IC bypass study group, Barnett HJM, Sackett DL, Taylor DW, Peerless SJ, Haynes RB, Gates PC, et al. Failure of extracranial-intracranial arterial bypass to reduce the risk of ischemic stroke. Results of an international randomized trial. The EC/IC bypass study group. *N Engl J Med.* 1985;313:1191–200.
  50. The EC/IC bypass study group, Haynes RB, Taylor DW, Mukherjee J, Sackett DL, Cote R, Meguro K, et al. The international cooperative study of extracranial/intracranial arterial anastomosis (EC/IC bypass study): methodology and entry characteristics. The EC/IC bypass study group. *Stroke.* 1985;16:397–406.
  51. Hennerici M, Hülsbömer HB, Rautenberg W, Hefter H. Spontaneous history of asymptomatic internal carotid occlusion. *Stroke.* 1986;17:718–22.

52. Hankey GJ, Warlow CP. Prognosis of symptomatic carotid occlusion: an overview. *Cerebrovasc Dis.* 1991;1:245–56.
53. Derdeyn CP, Yundt KD, Videen TO, Carpenter DA, Grubb Jr RL, Powers WJ. Increased oxygen extraction fraction is associated with prior ischemic events in patients with carotid occlusion. *Stroke.* 1998;29:754–8.
54. Vorstrup S. Tomographic cerebral blood flow measurements in patients with ischemic cerebrovascular disease and evaluation of the vasodilatory capacity by the acetazolamide test. *Acta Neurol Scand.* 1988;114(Suppl):1–48.
55. Yonas H, Smith HA, Durham SR, Pentheny SL, Johnson DW. Increased stroke risk predicted by compromised cerebral blood flow reactivity. *J Neurosurg.* 1993;79:483–9.
56. Yonas H, Pindzola RR. Physiological determination of cerebrovascular reserves and its use in clinical management. *Cerebrovasc Brain Metab Rev.* 1994;6:325–40.
57. Gotoh F, Meyer JS, Tomita M. Carbonic anhydrase inhibition and cerebral venous blood gases and ions in man. Demonstration of increased oxygen availability to ischemic brain. *Arch Intern Med.* 1966;117:39–46.
58. Okazawa H, Yamauchi H, Sugimoto K, Toyoda H, Kishibe Y, Takahashi M. Effects of acetazolamide on cerebral blood flow, blood volume and oxygen metabolism: a PET study with healthy volunteers. *J Cereb Blood Flow Metab.* 2001;21:1472–9.
59. Kuroda S, Kamiyama H, Abe H, Houkin K, Isobe M, Mitsumori K. Acetazolamide test in detecting reduced cerebral perfusion reserve and predicting long-term prognosis in patients with internal carotid artery occlusion. *Neurosurgery.* 1993;32:912–8.
60. Webster MW, Makaroun MS, Steed DL, Smith HA, Johnson DW, Yonas H. Compromised cerebral blood flow reactivity is a predictor of stroke in patients with symptomatic carotid artery occlusive disease. *J Vasc Surg.* 1995;21:338–44. discussion 344–345.
61. Kuroda S, Houkin K, Kamiyama H, Mitsumori K, Iwasaki Y, Abe H. Long-term prognosis of medically treated patients with internal carotid or middle cerebral artery occlusion: can acetazolamide test predict it? *Stroke.* 2001;32:2110–6.
62. Markus H, Cullinane M. Severely impaired cerebrovascular reactivity predicts stroke and TIA risk in patients with carotid artery stenosis and occlusion. *Brain.* 2001;124:457–67.
63. Ogasawara K, Ogawa A, Yoshimoto T. Cerebrovascular reactivity to acetazolamide and outcome in patients with symptomatic internal carotid or middle cerebral artery occlusion: a xenon-133 single-photon emission computed tomography study. *Stroke.* 2002;33:1857–62.
64. Ogasawara K, Ogawa A, Terasaki K, Shimizu H, Tominaga T, Yoshimoto T. Use of cerebrovascular reactivity in patients with symptomatic major cerebral artery occlusion to predict 5-year outcome: comparison of xenon-133 and iodine-123-IMP single-photon emission computed tomography. *J Cereb Blood Flow Metab.* 2002;22:1142–8.
65. Hasegawa Y, Yamaguchi T, Tsuchiya T, Minematsu K, Nishimura T. Sequential change of hemodynamic reserve in patients with major cerebral artery occlusion or severe stenosis. *Neuroradiology.* 1992;34:15–21.
66. Yokota C, Hasegawa Y, Minematsu K, Yamaguchi T. Effect of acetazolamide reactivity and long-term outcome in patients with major cerebral artery occlusive diseases. *Stroke.* 1998;29:640–4.
67. Yonas H, Pindzola RR, Meltzer CC, Sasser H. Qualitative versus quantitative assessment of cerebrovascular reserves. *Neurosurgery.* 1998;42:1005–10. discussion 1011–1012.
68. Okazawa H, Tsuchida T, Kobayashi M, Arai Y, Pagani M, Isozaki M, Yonekura Y. Can reductions in baseline CBF and vasoreactivity detect misery perfusion in chronic cerebrovascular disease? *Eur J Nucl Med Mol Imag.* 2007;34:121–9.
69. Mountz JM, Liu HG, Deutsch G. Neuroimaging in cerebrovascular disorders: measurement of cerebral physiology after stroke and assessment of stroke recovery. *Semin Nucl Med.* 2003;33:56–76.
70. Liu HG, Mountz JM. F-18 FDG brain positron emission tomography and Tl-201 early and delayed SPECT in distinguishing atypical cerebral tumor from cerebral infarction. *Clin Nucl Med.* 2003;28:241–2.
71. Feeney DM, Baron JC. Diaschisis. *Stroke.* 1986;17:817–30.
72. Herold S, Brown MM, Frackowiak RS, Mansfield AO, Thomas DJ, Marshall J. Assessment of cerebral haemodynamic reserve: correlation between PET parameters and CO<sub>2</sub> reactivity measured by the intravenous 133 xenon injection technique. *J Neurol Neurosurg Psychiatry.* 1988;51:1045–50.
73. Ito H, Kanno I, Shimosegawa E, Tamura H, Okane K, Hatazawa J. Hemodynamic changes during neural deactivation in human brain: a positron emission tomography study of crossed cerebellar diaschisis. *Ann Nucl Med.* 2002;16:249–54.
74. Astrup J, Siesjo BK, Symon L. Thresholds in cerebral ischemia – the ischemic penumbra. *Stroke.* 1981;12:723–5.
75. Baron JC. Positron tomography in cerebral ischemia. A review. *Neuroradiology.* 1985;27:509–16.
76. Raynaud C, Rancurel G, Samson Y, Baron JC, Soucy JP, Kieffer E, et al. Pathophysiologic study of chronic infarcts with I-123 isopropyl iodo-amphetamine (IMP): the importance of periinfarct area. *Stroke.* 1987;18:21–9.
77. Seitz RJ, Azari NP, Knorr U, Binkofski F, Herzog H, Freund HJ. The role of diaschisis in stroke recovery. *Stroke.* 1999;30:1844–50.
78. Karbe H, Kessler J, Herholz K, Fink GR, Heiss WD. Long-term prognosis of poststroke aphasia studied with positron emission tomography. *Arch Neurol.* 1995;52:186–90.

79. Cappa SF, Perani D, Grassi F, Bressi S, Alberoni M, Franceschi M, et al. A PET follow-up study of recovery after stroke in acute aphasics. *Brain Lang.* 1997;56:55–67.
80. Carmichael ST, Tatsukawa K, Katsman D, Tsuyuguchi N, Kornblum HI. Evolution of diaschisis in a focal stroke model. *Stroke.* 2004;35:758–63.
81. Clarke S, Assal G, Bogousslavsky J, Regli F, Townsend DW, Leenders KL, et al. Pure amnesia after unilateral left polar thalamic infarct: topographic and sequential neuropsychological and metabolic (PET) correlations. *J Neurol Neurosurg Psychiatry.* 1994;57:27–34.
82. Stenset V, Grambaite R, Reinvang I, Hessen E, Cappelen T, Bjornerud A, et al. Diaschisis after thalamic stroke: a comparison of metabolic and structural changes in a patient with amnesic syndrome. *Acta Neurol Scand Suppl.* 2007;187:68–71.
83. Heiss WD, Emunds HG, Herholz K. Cerebral glucose metabolism as a predictor of rehabilitation after ischemic stroke. *Stroke.* 1993;24:1784–8.
84. Herholz K, Heiss WD. Functional imaging correlates of recovery after stroke in humans. *J Cereb Blood Flow Metab.* 2000;20:1619–31.
85. Karbe H, Szelies B, Herholz K, Heiss WD. Impairment of language is related to left parieto-temporal glucose metabolism in aphasic stroke patients. *J Neurol.* 1990;237:19–23.
86. Heiss WD, Thiel A, Kessler J, Herholz K. Disturbance and recovery of language function: correlates in PET activation studies. *Neuroimage.* 2003;20(Suppl 1):S42–9.